Electrochemistry Communications 10 (2008) 1272–1275

Contents lists available at ScienceDirect

Electrochemistry Communications

journal homepage: www.elsevier.com/locate/elecom

Thermophoretic deposition of palladium aerosol nanoparticles for electroless micropatterning of copper

Jeong Hoon Byeon [a], Ki Young Yoon [b], Yee Kyeong Jung [b], Jungho Hwang [b,c,*]

[a] Digital Printing Division, Samsung Electronics Co., Ltd., Suwon 443-742, Republic of Korea
[b] School of Mechanical Engineering, 134 Shinchon-dong, Seodaemun-gu, Yonsei University, Seoul 120-749, Republic of Korea
[c] Yonsei Center for Clean Technology, Yonsei University, Seoul 120-749, Republic of Korea

ARTICLE INFO

Article history:
Received 8 June 2008
Received in revised form 21 June 2008
Accepted 24 June 2008
Available online 29 June 2008

Keywords:
Site-selective catalytic activation
Palladium aerosol nanoparticles
Electroless copper deposition
Micropatterning

ABSTRACT

A method for catalytic activation was introduced by producing palladium aerosol nanoparticles via spark generation and then thermophoretically depositing the particles onto a flexible polyimide substrate through a hole in pattern mask, resulting in a line (24 μm in width) and a square (136 μm × 136 μm) patterns. After annealing, the catalytically activated substrate was placed into a solution for electroless copper deposition. Finally, copper micropatterns of a line (35 μm in width) and a square (165 μm × 165 μm) were formed only on the activated regions of the substrate. Both patterns had the height of 1.6 μm.

1. Introduction

Microscale metallic patterns on various types of surfaces are of prime importance in many fields of technology, and enable the rapidly progressing miniaturization of components [1,2]. Copper is an attractive interconnect material for use in high density packaging and ultra-large scale integrated (ULSI) devices since it offers the advantages of low resistivity, high electromigration resistance and high melting point [3]. Since vapor deposition processes for fabrication of copper are very expensive and relatively slow despite the high quality of films achieved, it appears that electrochemical deposition of copper is the leading technology, as it offers low cost and fast deposition at low processing temperature [4]. One of the most widely used electrochemical deposition techniques for the fabrication of micro- and nano-patterned copper structures on substrates is the electroless deposition (ELD) [4–8] of copper, which is an important process widely used in microelectronics, packaging, and storage technologies to fabricate, for example, circuit lines in printed circuit board manufacturing, chip-level metal interconnects and contacts, and thin metal etch masks [9]. ELD on a substrate uses a pre-existing pattern of a catalytic species (palladium and platinum, etc.) to form the desired metal pattern [10]. In principle, since nucleation and growth are promoted in areas covered with a catalyst, preferential metallization can be easily controlled on to the desired surfaces [11]. Therefore, the quality in site-selective surface activation using catalyst particles significantly dominates the resolution of the metal pattern [10].

Aerosol catalysis is shown to be a powerful tool for investigating the catalytic properties of freshly formed nanoparticles in situ and without substrate interference [12]. Recently, Byeon et al. [13] reported a strategy for site-selective catalytic activation by producing metal aerosol nanoparticles via spark generation [14,15]. They enhanced the deposition of platinum aerosol particles vertically impinging onto a flexible polyimide (PI) substrate by controlling the thermophoresis, which is a physical phenomenon in which aerosol particles [16,17], subjected to a temperature gradient, move from high- to low-temperature zones of the gas. Without any chemical pretreatment, they were able to reproduce a selective deposition of particles on the PI substrate through a pattern hole. After annealing, the catalytically activated PI substrate was immersed in a silver ELD solution, resulting in the coating of silver on the selected spots of the PI substrate.

2. Experimental

ELD of copper was tested with the vertical flow configuration for catalytic activation, as suggested by Byeon et al. [13]. The results for palladium aerosol activation and copper ELD are shown in Fig. 1. Since the results were relatively poor compared to those of Byeon et al. [13], in this communication, a horizontal configuration shown in Fig. 2a was chosen instead of the vertical

* Corresponding author. Address: School of Mechanical Engineering, 134 Shinchon-dong, Seodaemun-gu, Yonsei University, Seoul 120-749, Republic of Korea. Tel.: +82 2 2123 2821; fax: +82 2 312 2821.
E-mail address: hwangjh@yonsei.ac.kr (J. Hwang).

1388-2481/$ - see front matter © 2008 Elsevier B.V. All rights reserved.
doi:10.1016/j.elecom.2008.06.025

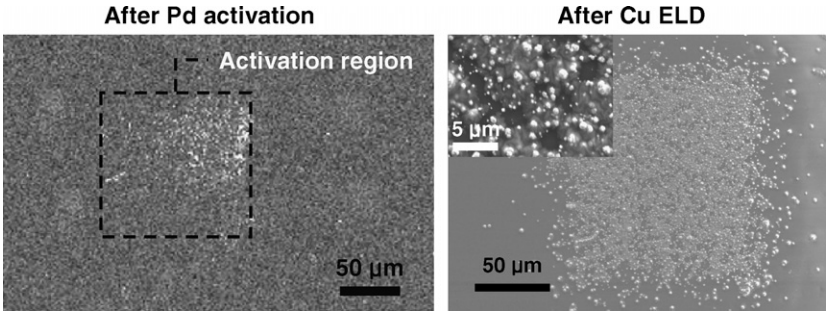

Fig. 1. Results of palladium aerosol activation and copper ELD using vertical activation system.

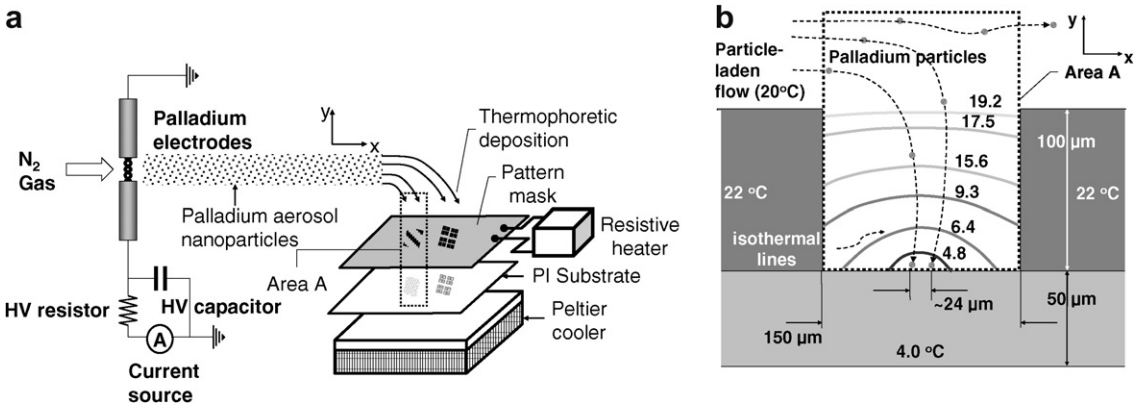

Fig. 2. (a) Overview of site-selective aerosol activation. (b) Temperature distribution inside the area *A* of Fig. 2a.

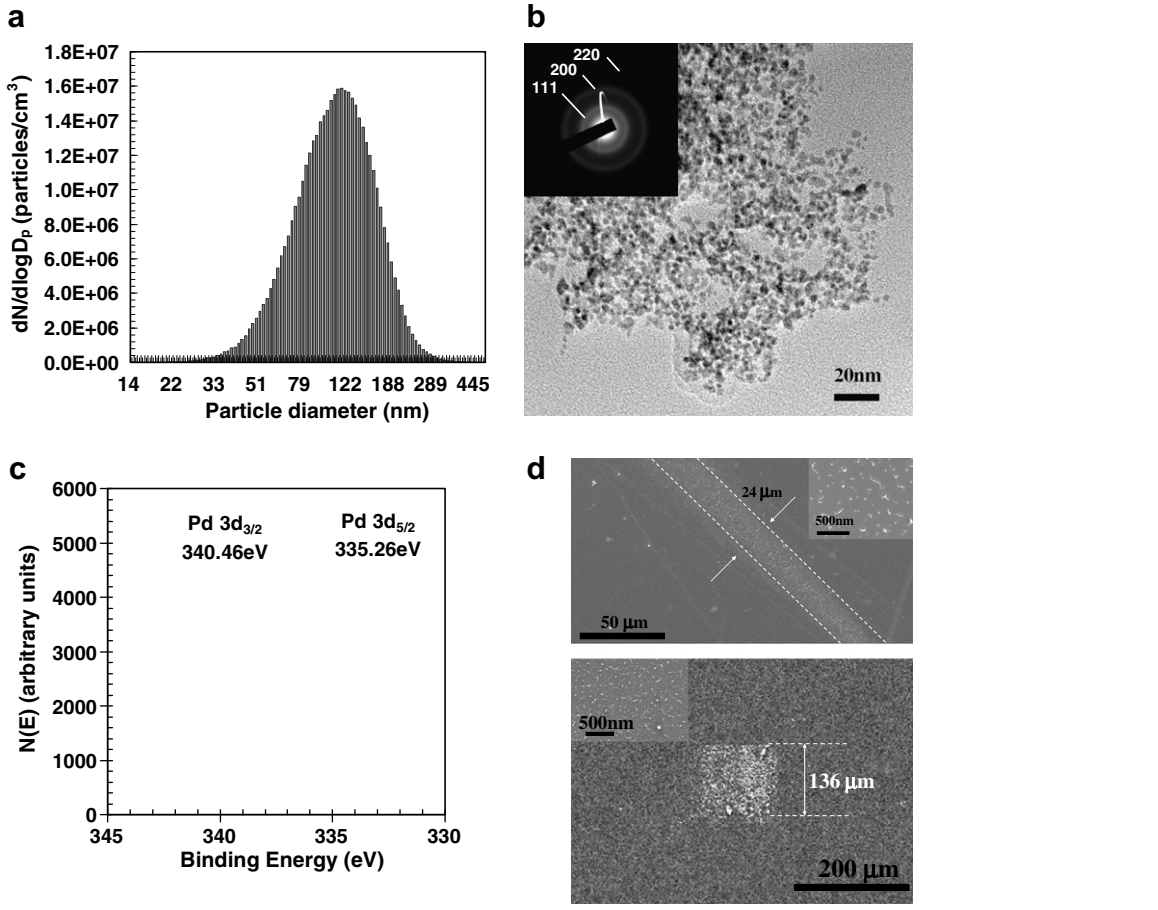

Fig. 3. Particle characterization of catalytic aerosol activation. (a) Particle size distribution of spark generated aerosol nanoparticles. (b) HRTEM image and SAED pattern (inset) of spark generated particles. (c) XPS profile of spark generated particles. (d) FESEM images of line and square patterns in PI substrate.

one to enhance spatial uniformity of catalytic activation and thus the quality of final copper patterns. The palladium aerosol nanoparticles were generated via spark discharge and carried by N_2 gas to a PI substrate through a hole in pattern mask (150 μm width × 100 μm depth for line pattern, 400 μm width × 400 μm length × 100 μm depth for square pattern) for a duration of 15 min. In the experiments, commercially available PI films (Kapton™, Dupont) having a 50 μm thickness were used as the substrates. A spark was generated between two identical palladium rods (diameter: 3 mm, length: 100 mm) inside a reactor under a pure nitrogen environment at standard temperature and pressure (STP) [18]. The flow rate of the nitrogen gas, which was controlled by a mass flow controller, was set at 60 mL/min. The electrical circuit specifications were as follows: resistance of 0.5 MΩ, capacitance of 10 nF, loading current of 2 mA, applied voltage of 2.8 kV, and frequency of 667 Hz. While the temperature of the particle-laden flow was kept at 20 °C, the temperatures of the stainless steel mask and PI substrate were kept at 22 °C (for preventing unwanted deposition of the particles onto the mask via thermophoresis) and 4 °C (for enhancing the deposition of the particles onto the PI substrate via thermophoresis) through the use of a resistive heater and a Peltier cooler, respectively. To understand the effect of thermophoresis on particle deposition, velocities and temperatures of the particle-laden flow were calculated using a commercial computational fluid dynamics (CFD) code (Fluent 6.3) with a finite volume grid containing approximately 50,000 cells. As shown in Fig. 2b, the particles were detached from the horizontal flow streamlines and deposited on the PI substrate by thermophoresis due to the temperature distribution inside the dotted area A in Fig. 2a.

Two solutions were mixed and used for the ELD solution. Solution A contained 3 g of $CuSO_4$, 14 g of sodium potassium tartrate (Rochelle salt), and 4 g of NaOH in 100 mL of deionized water. Solution B was an aqueous formaldehyde solution (37.2 wt%). The two solutions A and B were mixed in a 10:1 (v/v) ratio and the activated PI substrate was then immersed into the mixture so that copper particles would be coated on the activated sites. The PI substrate was rinsed with deionized water after it was removed from the ELD solution to remove the residual and then set aside to dry.

3. Results and discussion

Fig. 3a shows the size distribution of spark generated aerosol nanoparticles measured using a scanning mobility particle sizer

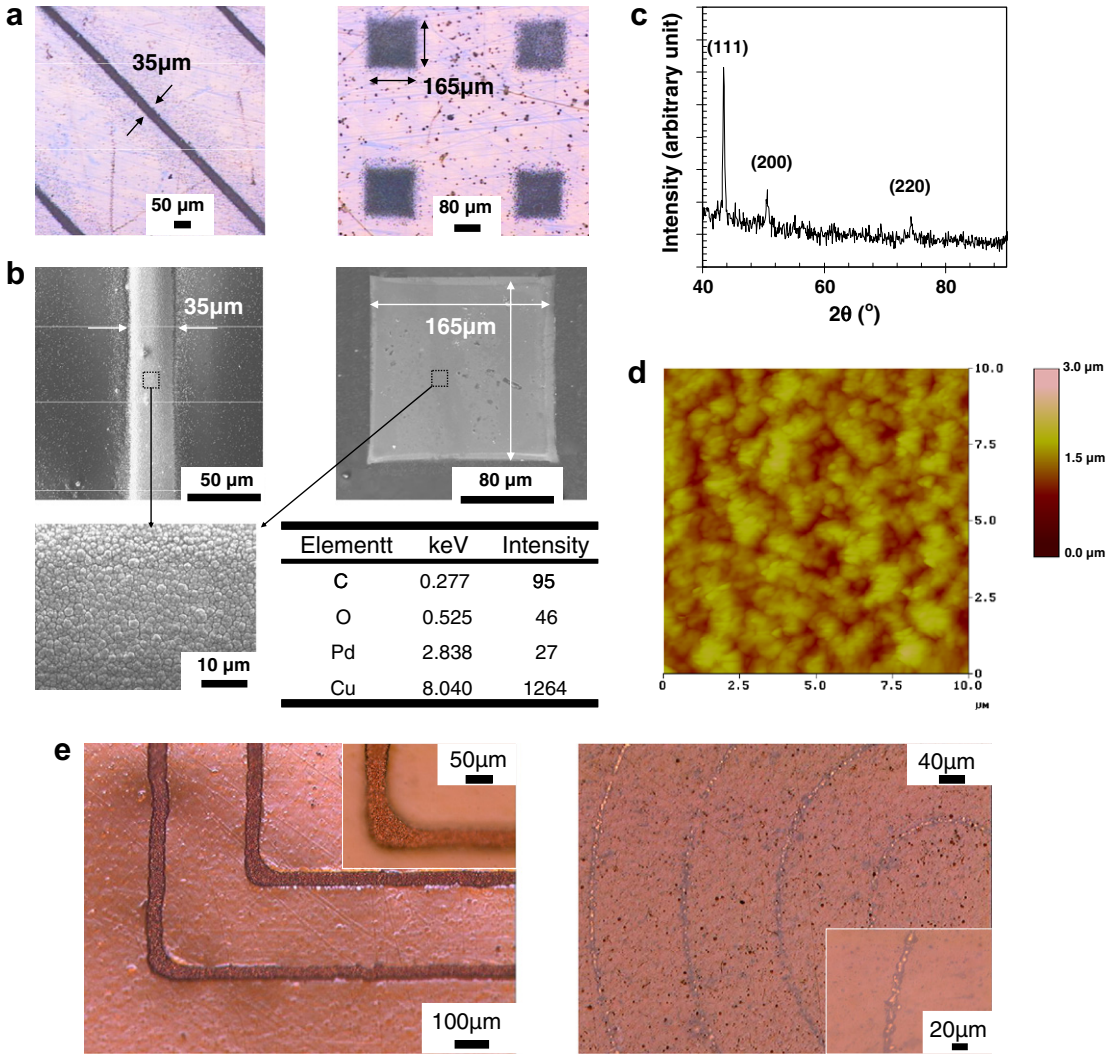

Fig. 4. Results of copper ELD. (a) Optical microscopy images of copper patterns (left: slanting lines, right: square arrays). (b) FESEM micrographs corresponding to the optical microscopy images with high-magnitude FESEM image and EDX data. (c) XRD profile. (d) 2D AFM profile. (e) Other copper micropatterns using different pattern masks. Angled-line array (left: 32 μm in width). Circled-line array (right: 8 μm in width).

(SMPS Custom, TSI) system. The geometric mean diameter and geometric standard deviation were 108.7 nm and 1.5, respectively. The total number concentration was 6.9×10^6 particles/cm^3. The high resolution transmission electron microscopy (HRTEM, JEM-3010) image (Fig. 3b) reveals that the particles were agglomerates of several primary particles (each ~28 Å in diameter). Fig. 3b also shows the selected area electron diffraction (SAED) pattern corresponding to the HRTEM micrograph. The pattern had diffraction lines showing [1 1 1] and [2 0 0] reflections and a weak diffraction line showing [2 2 0] of the face-centered cubic (fcc) lattice for metallic palladium. The X-ray photoelectron spectroscopy (XPS, AXIS HIS, Kratos) profile (Fig. 3c) of the particles reveals that they were pure palladium. The binding energy (BE) doublet with the BEs for the Pd $3d_{5/2}$ and Pd $3d_{3/2}$ peak components located at about 335 eV and 340 eV, respectively, are assigned to the Pd^0 species [19]. The field emission scanning electron microscopy (FESEM, JSM-6500F, JEOL) images (Fig. 3d) having a line and a square patterns show that the particles are spread out over the entire line and square. The FESEM images also show that the thermophoretic focusing of the particles (see Fig. 2b) resulted in a line (24 μm in width) and a square (136 μm width × 136 μm length), which are much narrower than those of the mask holes.

The catalytically activated PI substrate was then separated from the mask and annealed at 190 °C for 5 min in air to prevent detachment of the particles from the PI substrate. After annealing, the PI substrate was immersed into a copper ELD solution that resulted in the ELD of copper on the palladium nanoparticles of the PI substrate. The ELD of copper at 20 °C resulted in copper patterns appearing within 40 min. As shown in Fig. 4a, the copper ELD occurred only on the palladium nanoparticles, i.e., at the activated sites of the PI substrate. The palladium nanoparticles effectively acted as a seed to initiate the copper ELD. The copper patterns were wider than those of palladium patterns, as shown in Fig. 3d, because ELD is an isotropic process. The optical microscopy analysis revealed that patterns having 35 μm in width for a line and 165 μm × 165 μm for a square were obtained from the ELD (Fig. 4a). FESEM pictures corresponding to Fig. 4a show that copper particles were densely packed (Fig. 4b). From an energy dispersive X-ray spectroscopy (EDX, JED-2300, JEOL) analysis (also shown in Fig. 4b) it was found that the coated metal consisted mainly of copper, but contained a small amount of palladium as well as carbon and oxygen, which may have originated from the PI substrate. A X-ray diffractometry (XRD, RINT-2100, Rigaku) profile of the copper pattern shows that there exist three peaks located at $2\theta = 43.3$, 50.4, and 74.1° (Fig. 4c). These peaks correspond to the [1 1 1], [2 0 0], and [2 2 0] planes of the fcc phase for copper (JCPDS No. 04-0836). The average particle size evaluated according to Scherrer's formula was approximately 46 nm. Fig. 4d shows the 2D atomic force microscopy (AFM, NanoScope IIIa, Digital Instrument) profile obtained from Fig. 4b. The height and root-mean-square roughness were about 1.6 μm and 56 nm, respectively. Other copper patterns using different pattern masks were also demonstrated (Fig. 4e). Two stainless steel pattern masks having an angled-line array (150 μm in width) and a circled-line array (50 μm in width) were used to obtain copper patterns having the dimensions of 32 μm in width and 8 μm in width, respectively. Resistivities (ρ) of the copper line pattern (Fig. 4a) were calculated through the relationship $\rho = RA/L$, where R, A, L are the resistance, cross-sectional area, and length of the pattern, respectively. The average value of the resistivities was approximately 4.6 μΩ cm, which is almost comparable to the theoretical resistivity of bulk copper (1.7 μΩ cm).

4. Conclusions

Using our site-selective aerosol activation and ELD processes, it was possible to create stable and selective copper patterns with micrometer dimensions on a flexible PI substrate. Our processes were simple and environmentally benign, and can be applied in order to produce display electronics circuits, sensors, radio-frequency identification (RFID) transponders, and other microelectronic devices.

Acknowledgement

This study was supported by the Industrial Technology Development Project from the Ministry of Knowledge Economy.

References

[1] H. Jha, T. Kikuchi, M. Sakairi, H. Takahashi, Electrochem. Commun. 9 (2007) 1596.
[2] J. Feng, B. Cui, Y. Zhan, S.Y. Chou, Electrochem. Commun. 4 (2002) 102.
[3] P. Zhu, Y. Masuda, K. Koumoto, J. Mater. Chem. 14 (2004) 976.
[4] E.A. Speets, P. te Riele, M.A.F. van den Boogaart, L.M. Doeswijk, B.J. Ravoo, G. Rijnders, J. Brugger, D.N. Reinhoudt, D.H.A. Blank, Adv. Funct. Mater. 16 (2006) 1337.
[5] Y. Zhang, E. Balaur, S. Maupai, T. Djenizian, R. Boukherroub, P. Schmuki, Electrochem. Commun. 5 (2003) 337.
[6] I. Lee, P.T. Hammond, M.F. Rubner, Chem. Mater. 15 (2003) 4583.
[7] K.M. Metz, D. Divya, R.J. Hamers, J. Phys. Chem. C 111 (2007) 7260.
[8] L.A. Porter Jr., H.C. Choi, J.M. Schmeltzer, A.E. Ribbe, L.C.C. Elliott, J.M. Buriak, Nano Lett. 2 (2002) 1369.
[9] T.B. Carmichael, S.J. Vella, A. Afzali, Langmuir 20 (2004) 5593.
[10] W.K. Ng, L. Wu, P.M. Moran, Appl. Phys. Lett. 81 (2004) 3097.
[11] H. Asoh, F. Arai, S. Ono, Electrochem. Commun. 9 (2007) 535.
[12] A.P. Weber, M. Seipenbusch, G. Kasper, J. Phys. Chem. A 105 (2001) 8958.
[13] J.H. Byeon, J.H. Park, K.Y. Yoon, J. Hwang, Langmuir 24 (2008) 5949.
[14] J.H. Byeon, J.H. Park, J. Hwang, J. Aerosol Sci. 35 (2008), doi:10.1016/j.jaerosci.2008.05.006.
[15] R.L. Watters Jr., J.R. DeVoe, F.H. Shen, J.A. Small, R.B. Marinenko, Anal. Chem. 61 (1989) 1826.
[16] A. Messerer, R. Niessner, U. Pöschl, J. Aerosol Sci. 34 (2003) 1009.
[17] F. Zheng, Adv. Colloid Interface Sci. 97 (2002) 255.
[18] J.H. Byeon, B.J. Ko, J. Hwang, J. Phys. Chem. C 112 (2008) 3627.
[19] C.-L. Lee, L.-C. Kuo, Y.-C. Huang, Y.-W. Yen, Electrochem. Commun. 8 (2006) 697.